Experimental Study on Seismic Behavior of Conventional Concrete Bridge Bents

M.K. Bahrani[1], A. Vasseghi[2*], A. Esmaeily[3], and M. Soltani[4]

1. PhD Candidate of Structural-Earthquake Engineering, International Institute of Earthquake Engineering and Seismology (IIEES), Tehran, Iran
2. Assistant Professor, International Institute of Earthquake Engineering and Seismology, Tehran, Iran, * Corresponding Author; email: vasseghi@iiees.ac.ir
3. Associate Professor, Structural Engineering, Kansas State University, Manhattan, KS, USA
4. MSc. Graduate Student, Earthquake Structural-Engineering, International Institute of Earthquake Engineering and Seismology (IIEES), Tehran, Iran

ABSTRACT

This paper presents the results of an experimental study conducted to assess the seismic response of the commonly used multicolumn bridge bents constructed in Iran. Observing the real performance of the bent, capturing undesirable failure modes, and verifying current code requirements are the main goals of this study. A 30% scaled specimen was designed, constructed and tested under simulated earthquake loads. The results indicate that the joint failure and slippage of longitudinal column reinforcement within the joints are the predominant failure modes under lateral cyclic loading. Such failure modes adversely affect the energy-absorbing capacity by a significantly pinched hysteresis response. Slippage of the column's longitudinal bar is the main contributing factor for the pinched hysteresis response. Based on the test results, AASHTO requirements for development length of the column's longitudinal bars inside the cap-beam is unnecessarily long, and it can be reduced considering the confinement effects of transverse reinforcement. Test results also indicate that the displacement capacity of bridge bents calculated by the AASHTO approximate equation may be unconservative.

Keywords:
Bridge; Ductility;
Multicolumn bent;
Concrete;
Capacity assessment

1. Introduction

Most of the existing Reinforced Concrete (*RC*) bridges in Iran were designed for gravity and the simple lateral static loads [1]. Commonly supported by multiple column (multicolumn) pier bents, the bridges have simple spans or continuous concrete deck sitting on elastomer bearings. The bents are typically characterized by strong columns and weak cap-beams with some deficiencies in detailing and concrete confinement, especially in joints. These highway bridges are concentrated near big cities, and a significant portion of them are in mega city and the capital of Iran; Tehran. Bridges with similar deficiencies have experienced considerable damage in the recent earthquakes starting from the 1971 San Fernando to the 1994 Northridge, and a significant number of study has been carried out to improve seismic performance of the bridge piers [2-11].

Poorly detailed joints, especially exterior knee joints are the most vulnerable elements within the bridge bents under transverse lateral loading condition [12]. The concrete shear failure in the form of diagonal tension is a common mode of failure in joints with inadequate transverse reinforcement. The bond failure in the longitudinal bars has also been observed as another undesirable failure mode, especially where the main bars are not properly anchored [13]. A variety of strengthening techniques have been applied to joints and cap-beams. Construction of concrete or steel jackets is the most common type of retrofit strategies [12, 14, 15, 16].

Efforts are also made to define and qualify limit states and performance goals for bridge design and assessment [2, 17] similar to the studies on buildings [18]. Hose et al [19] initiated a performance assessment for bridge structures and proposed a 5-level

performance evaluation approach. The selection of the 5-level, described in Table (1), was based on over 15 years of large scale experimental studies performed in the structural laboratory at the University of California, San Diego.

While the *RC* bridges built in the late 1980's in Tehran, have not yet experienced a major earthquake [20-21], they are vulnerable to possible seismic events [22]. Depending on their importance, closure of the highway bridges may have a severe socio-economic impact, in addition to possible loss of property and life. It is critically important to make sure that highway bridges can survive the large ground motions of the inevitable upcoming earthquakes, and remain serviceable during and after a major seismic event. So, research on the behavior of such bridges under seismic loads is needed to detect major deficiencies and take required measures to ensure a dependable seismic response. This paper presents the results of an experimental study on a 30% scaled multicolumn bridge bent under simulated earthquake loading carried out at the structural engineering laboratory of the International Institute of Earthquake Engineering and Seismology (*IIEES*).

2. Test Specimen

A series of conventional highway bridge drawings and calculation notes for bridges constructed in late 1980 to early 1990 were studied to determine the specimen's configuration. This was limited to ordinary moderate span bridges with non-integrated multicolumn reinforced concrete bents, constructed within the aforesaid time period in Iran. Available bridge documents were investigated considering:

1) Frame cross section,
2) Column-cap flexural reinforcement ratio,
3) Confinement in the column and the joint area,
4) Column axial load ratio and,
5) Longitudinal column reinforcement anchorage length in the joints.

Table (2) lists the common specification of some of the selected bridges. Common design practice at the time of construction of these bridges did not require the control of the relative flexural capacity of column-cap, shear force transfer from the joint and designing capacity protected members. Contrary to the current seismic code requirements, they were designed with strong column and weak cap-beam where desirable plastic hinge and proper hierarchy would not form in the bents. Members were not designed for the shear demand based on flexural capacity. Hence, occurrence of an undesirable failure mechanism in these bridges during earthquake is expected.

Based on this investigation, counseling with expert bridge designers and considering typical reinforcement details, the specimen was designed based on a selected as-built prototype bent with the following specifications:

∨ Columns longitudinal reinforcement ratio was 1.3% and cap-beam flexural top and bottom rebar ratio was 0.3% and 0.2%, respectively.

∨ Column bars were anchored in the joint by 90 degrees inward standard hook.

∨ There was not sufficient transverse joint reinforcement around the longitudinal column bars. In many cases column spirals continued into the joint up to about 1/3 of the column diameter.

∨ The axial force on the columns was 6% of the section capacity $(A_g f_c')$.

Figure (1) shows the schematic of the test specimen and the reinforcement details. Because of

Table 1. Definition of 5 performance levels [19].

Level	Performance Level	Qualitative Performance Description	Quantitative Performance Description
I	Cracking	Onset of Hairline Cracks	Cracks Barely Visible
II	Yielding	Theoretical First Yield of Longitudinal Reinforcement	Crack Widths < 1mm
III	Initiation of Local Mechanism	Initiation of Inelastic Deformation. Onset of Concrete Spalling. Development of Diagonal Cracks	Crack widths 1-2mm. Length of Spalled Region > 1/10 Cross-Section Depth.
IV	Full Development of Local Mechanism	Wide Crack Widths/Spalling Over Full Local Mechanism Region	Crack Widths > 2mm. Diagonal Cracks Extend Over 2/3 Cross-Section Depth. Length of Spalled Region> 1/2 Cross-Section Depth.
V	Strength Degradation	Buckling of Main Reinforcement. Rupture of Transverse Reinforcement Crushing of Core Concrete	Crack Widths > 2mm in Concrete Core. Measurable Dilation> 5% of Original Member Dimension.

Table 2. Common specification of selected bridges.

Name	Kashani	Molla Sadra	Aramene	Mohajeran	Azadegan	Average	Test Specimen
Intersection	Kashani Hwy vs. Asia Blvd	Chamran Hwy vs. Molla sadra Ave.	Khavaran, Aramene Cemetery	Mohajeran vs Tooreh Intersection	Azadegan Hwy vs Tehran-Karaj Hwy		
Span *(m)*	16.5	15.5	19	19	20.5	18.4	
Column							
Diameter *(mm)*	1200	1200	1200	2000	1100	1329	350
Clear Height *(mm)*	6700	7000	6800	7600	7000	7086	2500
c/c Distance *(mm)*	4000	5000	6500	5200	4000	4814	1200
Longitudinal Steel	22T26	16T32	34T25	30T28	32T32		16T10
ρ_L	1.03	1.14	1.48	0.78	2.71	1.27	1.31
Hinge Transverse Steel	T16@70	T12@125	T12@65	T12@75	T12@15		T8@60
Type	Spiral	Hoop	Spiral	Spiral	Spiral		Spiral
ρ_V	0.24	0.08	0.14	0.08	0.69	0.42	0.24
Shear Transverse Steel	T10@150	T12@200	T12@200	T12@100	T12@200		T8@60
ρ_V	0.04	0.05	0.05	0.06	0.05	0.06	0.24
Cap Beam							
Section Depth *(mm)*	1000	1000	550	1200	1200	1058	300
Section Breadth *(mm)*	1750	1750	1500	2100	1600	1717	500
Top Steel	11T28	12T25	8T25	12T32	12T25		6T10
ρ_L	0.39	0.34	0.48	0.38	0.31	0.35	0.31
Bottom Steel	7T28	12T25	10T25	8T28	12T20		4T10
ρ_L	0.25	0.34	0.59	0.20	0.20	0.28	0.21
Transverse Steel	6T10@200	6T12@120	6T12@150	6T14@150	6T14@150		2.25T8@100
ρ_V	0.13	0.32	0.30	0.29	0.38	0.26	0.23
Joint							
Confinement Steel							
Applied Length *(mm)*	600	0	500	400		375	150
Diameter *(mm)*	16	0	12	12			8
Space *(mm)*	70	125	65	75			150
ρ_S	0.96	0.00	0.58	0.30		0.46	0.38
Col. Bar Develop. Length *(mm)*	850	850	450	400		638	240
Hook Length *(mm)*	600	500	400	400		475	100
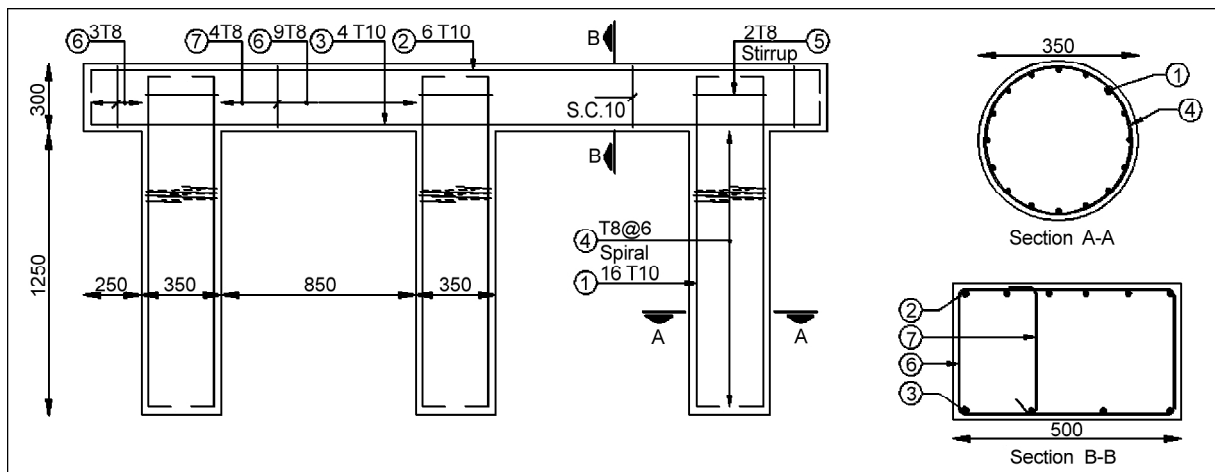
Figure 1. Specimen drawings: overall dimensions, sections, details and positions of reinforcements (units in mm).

the large size and weight of the actual bent, it was not feasible to test the entire bent in the laboratory. The available test facilities required simplification of the test specimen in a way that the test data would be a realistic representation of the performance of the actual bridge bent. The specimen was simplified by considering a pin connection at the column mid-height and modeling only the top portion of the bent. The prototype bent was scaled by 30% in dimensions while stresses remained constant, so that the axial load and the steel ratio were the same as the prototype. The cap-beam height was less than the column diameter and its flexural capacity with respect to the column was about 1/2 in positive and 2/3 in negative cap-beam moment. Consequently, the first plastic hinge would form in the cap-beam near the knee joint. The sum of the cap-beam flexural capacities on the two sides of the column exceeded the column flexural capacity at the tee joint. The yielding of the cap-beam was expected to precede the yielding of the column under the cap-beam positive moment. The cap-beam had an adequate shear capacity to develop the plastic hinge moments due to the common use of eight stirrup legs in the actual bridges and the same steel ratio in the specimen.

The material used for the specimen had the same properties as found in the actual construction. Standard cylindrical compression strength of the 28-day old concrete was $26MPa$ in the practice, where this value was 24 and $31MPa$ for the cap-beam and the column of the specimen, respectively. Longitudinal bars with grade *AIII* ($f_y = 400MPa$)

and transverse reinforcements with grade *AII* ($f_y = 300MPa$) were used in the specimen. The actual mechanical properties of the steel used in construction of the specimen are tabulated in Table (3).
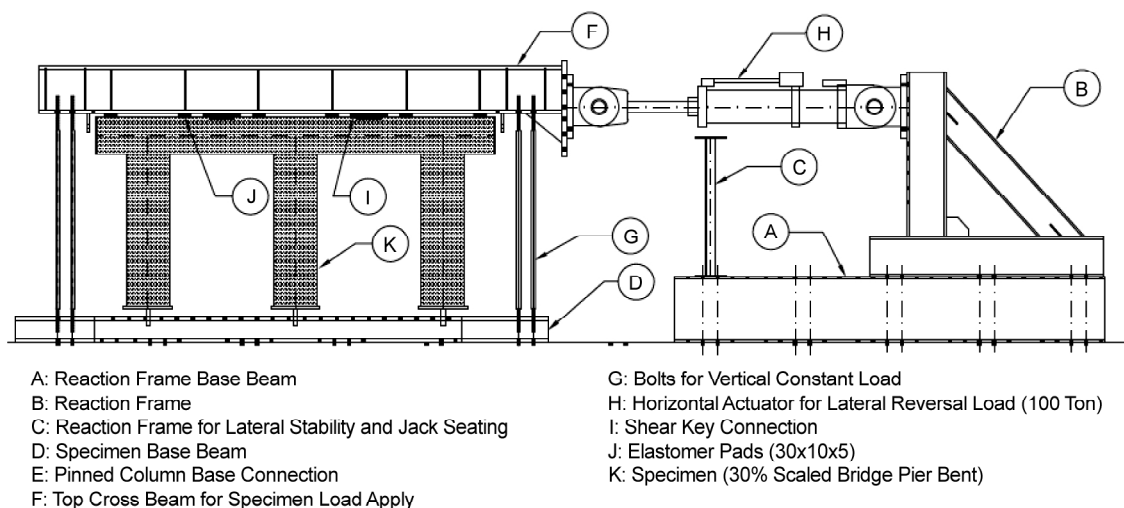
Table 3. Actual mechanical properties of the reinforcement used in the construction of the specimen.

Reinforcement Type	Yield Stress (MPa)	Ultimate Stress (MPa)	Ultimate Strain (%)
Longitudinal	521.5	697.3	14.3
Stirrups	352.3	543.7	12.47

3. Test Setup

Figure (2) shows the test setup for application of the gravity and seismic load on the specimen. Pinned base connections were modeled using two high-strength bolts, pre-installed in each of the columns. The gravity load was applied by pre-tensioning eight high-strength bolts connected to the cross beam by means of 16 elastomeric pads. These pads were used to reduce the fluctuation of the gravity loads during the lateral loading. The loads were transferred to the specimen through six bearing elastomers placed between the spreader steel cross beam and top surface of the cap-beam. The gravity load was controlled by monitoring the strain gauges installed on the bolts.

Representative earthquake lateral load was applied using $1000kN$ horizontal actuator, through a prescribed displacement path. The loading protocol

A: Reaction Frame Base Beam
B: Reaction Frame
C: Reaction Frame for Lateral Stability and Jack Seating
D: Specimen Base Beam
E: Pinned Column Base Connection
F: Top Cross Beam for Specimen Load Apply

G: Bolts for Vertical Constant Load
H: Horizontal Actuator for Lateral Reversal Load (100 Ton)
I: Shear Key Connection
J: Elastomer Pads (30x10x5)
K: Specimen (30% Scaled Bridge Pier Bent)

Figure 2. Test Setup and main components.

which is recommended by *ATC*-40 is shown in Figure (3). The displacement path consisted of three cycles at each level of displacement. Measurement instruments were linear variable differential transformers (*LVDT*) at the top and the base of the specimen and at locations with a critical displacement such as sliding of the cross beam on the specimen cap-beam. Strain-gauges were mounted on the longitudinal reinforcement of the column and the cap-beam.
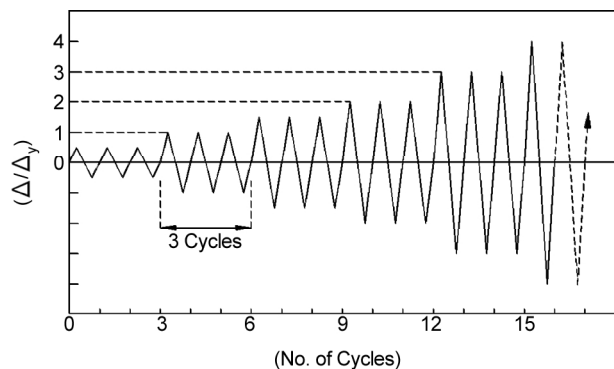

Figure 3. Applied displacement protocol.

The test started with a displacement amplitude less than the estimated yield point, in order to find the actual yield displacement. Monitoring the initial load-displacement behavior, the yield displacement was estimated about 24*mm* and the test continued using predetermined displacement pattern until significant strength deterioration happened.

3.1. Test Observation

3.1.1. Damage and Performance Levels

Damage propagation during the test and assigned performance levels are presented in this section. Predefined performance levels proposed by Hose et al [19] and presented in Table (1) are used for performance assignment. These levels are defined qualitatively based on the main damage propagation like hairline cracks, onset of spalling, bar buckling and also quantitatively based on crack width.

Performance level I: The bent behaved elastically with no significant degradation in the lateral strength at low displacement. Hairline flexural cracking initiated at stirrups' locations in the cap-beam at 0.88% drift ratio and then began to incline slightly in the next cycles. These cracks appeared at the bottom of the cap-beam near the exterior columns.

Vertical hairline cracks were observed in the joint area at 1.1% drift ratio, and flexural cracks were observed in the columns at 1.4% drift ratio. However, upon unloading, the cracks were closed and did not need repair. By increasing the displacement, hence loading magnitude, diagonal cracks appeared in the joints at 1.6% drift ratio and propagated quickly. Figure (4a) shows the crack pattern and damage at the performance level (I).

Performance level II: Yielding, initiated at 2.2% drift ratio by the longitudinal bar in the middle-column. Flexural cracks that had propagated up in the column showed increased inclination while the diagonal cracks at the joint propagated and widened. However, crack widths remained less than 1*mm* indicating that the repair was still possible and easy. At this level, flexural cracks in the cap-beam did not propagate and the strain in the longitudinal cap-beam bars was less than the yield value. Figure (4b) shows the crack pattern and damages at the performance level (II).

Performance level III: In the testing process, opening and widening of the cracks on the cap-beam near the exterior column started at 2.8% drift ratio. Since the longitudinal bars in the cap-beam did not yield, no crack-propagation was observed. However, just one main flexural crack was opened, which can be associated with the loss of the bond stress of the reinforcement, leading to a wide crack of the concrete at the joint region. This crack width was more than 2.5*mm* and remained open after unloading, requiring repair. Initiation of local mechanism happened at this level and was followed by the opening of a new wide crack in the middle-column and cap-beam interface due to the longitudinal bar slip at the joint. Strain gauges showed that the strain in the previous yielded longitudinal bars decreased due to the bar slippage. Onset of spalling started in the cap-beam during the third loading cycle of 2.8 % drift ratio.

Performance level IV: Spalling of the cover concrete started at the cap-beam, continued by increasing the lateral displacement, and expanded to the column faces. At 4.2% drift ratio, spalling was observed near the main wide cracks in the cap-beam and the column, indicating the absence of plastic hinge formation in the members and showing bar-slippage in both the cap-beams and the column. In this performance level, the local mechanism was fully developed, and an extensive crushing and

spalling of the compression face zones occurred. Very wide cracks measuring more than 5*mm* and 3 mm opened at the positive moment of the cap-beam near the exterior columns and at the column-cap interfaces, respectively. Figure (4c) shows the crack pattern and damages at the performance level (IV).

Performance level V: Further cyclic displacement of 5.6% drift ratio, led to significant lateral strength degradation. Diagonal crack widths at the joints and flexural cracks on the column were 2*mm*, and the main crack widths were more than 5*mm* on the cap-beam and column-cap interface. At this stage as an ultimate limit state, no spiral fracture, longitudinal bar buckling or spalling and crushing of core concrete was observed. Moreover, because of the slippage of the longitudinal column bars, spalling of concrete at the top surface of the cap-beam was observed. The crack pattern and damages at the performance level (V) is shown in Figure (4d).

3.2. Observed Behavior

The cyclic lateral force versus displacement response for the bent, along with the envelope profile and the performance points is shown in Figure (5). At 1.4% drift ratio, the force was 150*kN* and it remained constant during three repeated cycles. At 2.8% drift ratio, the force in the first cycle was 206*kN* which decreased by 11% to 184*kN* in the next two cycles. Increasing the displacement amplitude to 4.2% drift ratio, the force rose to the previously-reached maximum level of 205*kN* and in the similar manner, experienced 13% in-cycle degradation to 179*kN*. At this loading level, a slight dip in the force was observed, indicating the start of the failure mechanism. However, the significant drop in the lateral load capacity did not initiate until loading at 5.6% drift ratio in which the maximum force decreased 12% to 180*kN* and a huge in-cycle degradation of 17% and 26% was observed in the repeated second and third cycles, respectively.

a) Performance Level (I)
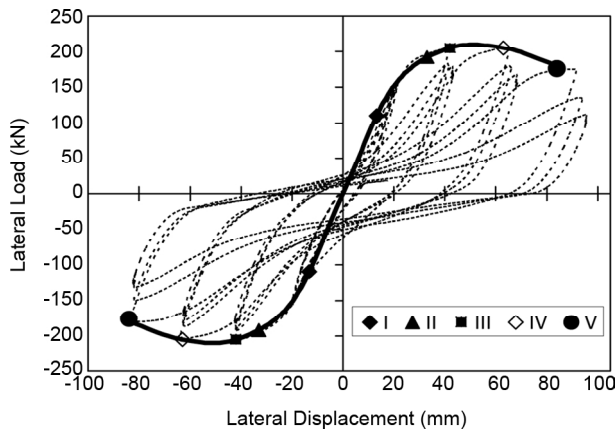

b) Performance Level (II)

(c) Performance Level (IV)

(d) Performance Level (V)

Figure 4. Crack pattern and damage observation at selected performance levels.

Figure 5. Different performance level points on the force-displacement response curve.

Figure 6. Comparison of proposed FEMA-356 and ASCE-41 backbone curves and derivation of ideal elasto-plastic curve based on ASCE-41 backbone.

Failure of the bent occurred during the second cycle at this ductility level where the 20% loss in lateral load capacity was registered [23]. According to Eurocode 8 [24] for ductile behavior, the global force-displacement relationship shall be reversible to ensure hysteretic energy dissipation at least over five repeated deformation cycles. Maximum drop of the resisting force at the ultimate displacement capacity shall not exceed 20% of the yield force. With the large degradation of lateral force in repeated cycles, the 4.2% drift ratio could be determined as ultimate displacement capacity.

The response envelope with symbols showing the performance levels is shown in the Figure (5). The failure occurred before the plastic hinges formed because of the bar slippage. In this figure, the bar slip is represented by a large amount of in-cycle lateral load degradation. Slippage of longitudinal bars was also identified by strain gauge data.

3.3. Behavior Idealization and Ultimate Displacement Capacity

The backbone curve was defined in *FEMA* 356 [23] through the intersection of the first cycle for the ith deformation step and second cycle at the $(i-1)^{th}$ deformation step. This type of backbone relations exaggerated the rate of the strength degradation, and it can result in an over-estimation of the earthquake deformation demands [25], especially where large in-cycle strength loss occurs. In the update to *ASCE/SEI* 41 [26] Concrete Provisions, Elwood et al [27] proposed that the backbone curves should be drawn through each point of peak displacement during the first cycle of each

increment of deformation. Both types of backbone curves were derived from the hysteresis response and are shown in Figure (6).
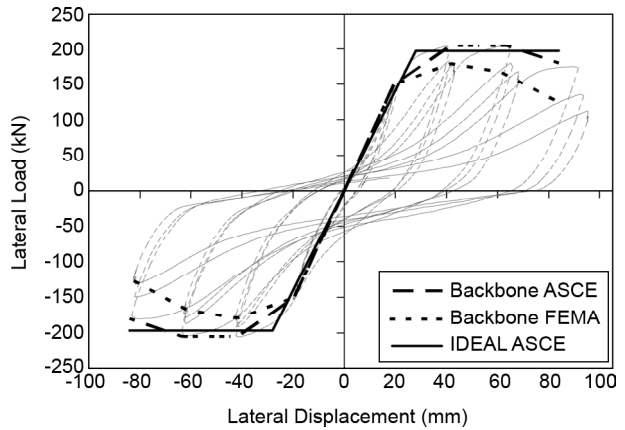
4. Discussion of the Test Results

4.1. Column Bar Anchorage and Confinement in the Joint

Column longitudinal bars were anchored in the cap-beam of the as-built specimen, by $240mm$ length and confined with two spirals at the joint area. According to AASHTO [28], the basic development length in the hooked-bar should be more than $l_{dh} = 100d_b / \sqrt{f'_c}$. This length should be increased by $f_y / 420$ for $f_y \geq 420MPa$ and it may be reduced by a factor of 0.7 when the concrete cover is more than $64mm$. Also, it may be multiplied by the modification factor of 0.8, if reinforcement is enclosed within the specified transverse stirrups. The longitudinal steel development length should be multiplied by a factor of 1.25 in the column-cap connections ensuring full yield of reinforcements, considering steel over-strength. Hence, according to AASHTO [28], without considering seismic provisions, the required development length is calculated as follows:

$$l_{dh} = (1.25)(0.7)(500/420)(100*10/\sqrt{22.5} = 220m \quad (1)$$

The required development length is less than the existing length of $240mm$. Also, the basic development length in compression, l_{db}, equals to the maximum of $0.24d_b f_y / \sqrt{f'_c}$ or $0.044d_b f_y$, and it may be multiplied by a modification factor of 0.75,

if reinforcement is enclosed within the spiral transverse reinforcement. The length could not be reduced in the case of hooked reinforcement.

$$l_{db} = (0.24 * 10 * 500 / \sqrt{22.5}) = 253mm \qquad (2)$$

For the test specimens, the required development length in compression is $253mm$, which is just 5% more than the existing $240mm$ development length.

It may be predicted that the potential of the longitudinal bar slippage in compression may be more than tension. Strain gauges showed that the first yield of the column bars occurred in tension and in the reversal loading, while the first bar slip happened in compression, which can be attributed to the lack of development length in compression. On the other hand, the existence of 90 degrees hook at the end of the bars, could have affected the anchorage of the bars in tension, but it was not effective in compression.

Caltrans [29] requirement of enough cap-beam depth to develop the column longitudinal reinforcement highlights the importance of column bar anchorage in the joint. If the criteria for adequacy of the joint shear reinforcement, i.e. the minimum bar spacing requirements and confinement along the development length, are met; the anchorage for longitudinal column bars developed into the cap-beam for seismic loads should not be less than $l_{ac} = 24d_b = 240mm$, which was exactly the existing development length in the specimen. This length judiciously cannot be reduced by adding hooks. The volumetric ratio of the confinement steel along l_{ac} should not be less than the value required for column plastic hinges. But, if the joint region is not confined by solid adjacent members, it should not be less than $\rho_s = 0.6\rho_l D_c / l_{ac} = 0.01$. The main idea is that

quite short development lengths might be possible, provided that the core is properly confined by transverse hoops or spirals [30]. In the as-built specimen, there were only two spirals at $120mm$ spacing at the development length of $240mm$, while available volumetric ratio of the confinement steel, ρ_s, was equal to 0.005, approximately about 50% of the required ratio. In spite of the fact that the required development length was satisfied, the required bond stress could not be developed, and bar slippage was observed due to deficiency of the confinement steel.

AASHTO [31] seismic design provisions require that the column longitudinal reinforcement should be extended into the cap-beams as close as practically possible to the opposite face of the cap-beam. The anchorage length for longitudinal column bars developed into the cap-beam for seismic loads should satisfy $l_{db} = 0.79d_b f_{ye} / \sqrt{f'_c} = 868mm$. This value is 4 times of the required length calculated by AASHTO [28] for non-seismic design, and about 3.6 times of the value suggested by Caltrans and the existing anchorage length in the test built specimen. It is almost difficult to accommodate such anchorage length within the normal superstructure depths. Also, this value cannot be reduced by adding hooks or mechanical anchorages. AASHTO [31] does not include the effect of the confinement reinforcement on the anchorage length reduction. Brief review of development length requirements is summarized in Table (4).

Looking at test measurements, strain gauge records showed that longitudinal bar strains exceeded the yield value and bar slippage occurred at a strain slightly more than the yield. It could be assumed that anchorage of the longitudinal bar was adequate

Table 4. Brief review of development length requirements in different codes compared with present specimen.

Requirements	Development Length (mm)			Spiral Volumetric Ratio	Description
	Tension	Compression	Ratio		
Present Specimen	240	240	1.00	0.0054	-
AASHTO [28] (No-Seismic)	220	253	1.05	-	Hooks considered in length reduction in tension. Confinement steel not a requirement but its effect is considered once present.
AASHTO [31] (Seismic)	868	-	3.62	0.0087	Same development length for tension and compression. Effects of hooks not considered in length reduction except for SDC C. Confinement steel is required.
Caltrans [29]	240	-	1.00	0.0101	Same development length for tension and compression. Effects of hooks not considered in length reduction Confinement steel is determined based on the provided development length.

for reinforcement to be yielded, and it was not adequate for the over-strength of steel tensile strength due to the formation of plastic hinge. Hence, it can be stated that AASHTO [31] requirement for development length may be unnecessarily large.

Upon observation of high bond stress of $2.5/\sqrt{f_c'}$ in column-cap joints, Priestley et al [32] recommends $l_{db} = 0.3 d_b f_{ye}/\sqrt{f_c'}\, mm$ for column bar anchorage length which corresponds to $330\,mm$ for the test specimen. This anchorage length is suggested for the joints with adequate transverse reinforcement or with adjacent members which is less than half of the expression recommended by AASHTO [31].

4.2. Ultimate Displacement Capacity

Each bridge structure should be categorized to predefined seismic response by damage level and ductility demand, μ_D, which is introduced for that damage level. For example, conventional ductile response for life safety of bridges in high seismic hazard zones, e.g. Seismic Design Category *D* (*SDC D*), is required, and the ductility demand is $4 \le \mu_D \le 6$. For limited ductile response, *SDC B* and *SDC C*, ductility demand is limited to $\mu_D \le 4$. Development of plastic mechanism should be clearly defined in both cases and inelastic actions should be restricted to flexural plastic hinge in columns. Seismic design of bridges involved comparing the displacement demand, D_D, with displacement capacity, D_C, of the structure and each bridge bent and each member shall satisfy Eq. (3).

$$D_D \le D_C \tag{3}$$

Detailed push-over analysis is required to calculate displacement capacity for *SDC D* bridge bents. However, for *SDC B* and *SDC C* bridges, the displacement capacity may be estimated from the following approximation equations.

$$D_C = 0.12 H_o(-1.27 \ln(x) - 0.32) \ge 0.12 H_o,$$
$$\text{for } SDC\ B \tag{4}$$

$$D_C = 0.12 H_o(-2.32 \ln(x) - 1.22) \ge 0.12 H_o,$$
$$\text{for } SDC\ C \tag{5}$$

where H_o is column clear height, $x = B_o/H_o$, and B_o is the column diameter. These simple equations are primarily intended for determining displacement capacities of bridges with single and multiple column reinforced concrete piers. These values are also calibrated for columns with $H_o \ge 4.6m$ where preferred plastic hinging mechanism is anticipated. Thus, in the bents with no desired plastic hinge mechanism, like joint shear failure or cap-beam weakness, these equations may require some corrections. For the specimen in this study:

$$x = 350/1250 = 0.28 \tag{6}$$

$$D_C = 0.12 H_o(-2.32 \ln(0.28) - 1.22) =$$
$$0.208 H_o = 0.17 H_{bent} \tag{7}$$

The calculated drift ratio of 17% largely overestimates the observed ultimate drift ratio of 5.6%. This is mainly due to the undesirable failure mode of the joint.

For common highway bridge bents, if the column diameter is considered to be $1.2m$ and column clear height are considered to be $5m$ for short bents and $10m$ for tall bents, the value of x lies between 0.48 and 0.24, and the displacement capacity lies between $0.06 H_o$ and $0.25 H_o$ respectively. It can be found that for short bents, the displacement capacity will be reasonable while for very tall bents with slender columns, it will lead to overestimated large displacement capacities. For short columns, the minimum height limitation of $4.6m$ was applied in the code, but for tall columns, application of a limit on maximum column height or modification of the equation may be required to restrict the aforesaid large values. Hence defining a valid range for the x parameter is necessary as it was done for the lower limit in the column clear height.

5. Conclusions

A 30% scaled specimen representing a commonly used bridge bent with deficiencies in the confinement and the shear reinforcement of joints, is studied experimentally and the main findings are as follows:

∨ Longitudinal bar slippage within the joint was the main source of degradation and loss of lateral strength.

∨ A large amount of in-cycle degradation was observed after longitudinal bars slippage.

∨ Out-cycle degradation did not occur prior to a drift ratio of 5.6%.

∨ AASHTO [31] overestimates the development length for the column's longitudinal bars in the joint as it does not include for the positive effect

of the transverse reinforcement on the development length.

∨ The displacement capacity of the common bridge bents, calculated using the approximate equation proposed by AASHTO [31] could be unconservative especially for tall columns. In many cases, the calculated displacement capacity would be more than the maximum allowable ductility demand.

6. Acknowledgments

References

1. SLB (2000). Standard Load for Bridges, Office of the Deputy for Technical Affairs Bureau of Technical Affairs and Standards, Tehran, Iran.

2. Kawashima, K. and Unjoh, S. (1997). "The 1996 Seismic Design Specifications of Highway Bridges", *Workshop of Earthquake Engineering Frontiers in Transportation Facilities*, Buffalo, New York.

3. Lowes, L.N. and Moehle, J.P. (1995). "Seismic Behavior and Retrofit of Older Reinforced Concrete Bridge T-Joints", *Earthquake Engineering Research Center, EERC*, 95-99.

4. Mander, J.B. and Chen, S. (1995). "Seismic Retrofit Procedures for Reinforced Concrete Bridge Piers in the Eastern United States", NCEER Report.

5. Eberhard, M.O. and Marsh, M.L. (1997). "Lateral Load Response of Two Reinforced Concrete Bents", *ASCE Journal of Structural Engineering*, **123**(4), 461-468.

6. Ingham, J.M., Priestley, M.J.N., and Seible, F. (1998). "Cyclic Response of Bridge Knee Joints with Circular Columns", *Journal of Earthquake Engineering*, **2**(3), 357-391.

7. Sritharan, S., Priestley, M.J.N., and Seible, F. (1999). "Enhancing Seismic Performance of Bridge Cap-Beam-to-Column Joints Using Prestressing", *PCI Journal*, **44**(4), 74-91.

8. Sritharan, S., Priestley, M.J.N., and Seible, F. (2001). "Seismic Design and Experimental Verification of Concrete Multiple Column Bridge Bents", *ACI Structural Journal*, **98**(3), 335-346.

9. Pulido, C., Saiid Saiidi, M., Sanders, D., Itani, A., and El-Azazy, S. (2004b). "Seismic Performance of Two-Column Bents - Part I: Retrofit with Carbon Fiber-Reinforced Polymer Fabrics", *ACI Structural Journal*, **101**(4), 558-568.

10. Pulido, C., Saiid Saiidi, M., Sanders, D., Itani, A., and El-Azazy, S. (2004a). "Seismic Performance of Two-Column Bents - Part II: Retrofit with Infill Walls", *ACI Structural Journal*, **101**(5), 642-649.

11. Pantelides, C.P., Ward, J.P., and Reaveley, D.L. (2004). "Behavior of R/C Bridge Bent with Grade Beam Retrofit under Simulated Earthquake Loads", *Earthquake Spectra*, **20**(1), 91-118.

12. Mazzoni, S. and Moehle, J.P. (2001). "Seismic Response of Beam-Column Joints in Double-Deck Reinforced Concrete Bridge Frames", *ACI Structural Journal*, **98**(3), 259-269.

13. Pauley, T. and Priestley, M.J.N. (1992). "Seismic Design of Reinforced Concrete and Masonary Buildings", John Wiley & Sons, Inc., New York.

14. Priestley, M.J.N., Seible, F., and Anderson, D.L. (1993a). "Proof Test of a Retrofit Concept for the San Francisco Double-Deck Viaducts - Part 1: Design Concept, Detail and Model", *ACI Materials Journal*, **90**(5), 467-479.

15. Priestley, M.J.N., Seible, F., and Anderson, D.L. (1993b). "Proof Test of a Retrofit Concept for the San Francisco Double-Deck Viaducts - Part 2: Test Details and Results", *ACI Materials Journal*, **90**(6), 616-631.

16. Lubiewski, M., Silva, P., and Chen, G. (2006). "Seismic Retrofit of CISS Pile Bent Cap

Connections", University Transportation Center Program at the University of Missouri-Rolla, Report No. CIES 06-64.

17. Hose, Y.D., Silva, P.F., and Seible, F. (1999). "Performance Library of Concrete Bridge Components, Sub-assemblages and Systems under Simulated Seismic loads", Structural System Research Program, SSRP 99/08, University of California, San Diego.

18. SEAOC (1996). App. B: Conceptual Framework for Performance based Seismic Design, Vision 2000, Structural Engineering Association of California.

19. Hose, Y.D., Silva, P.F., and Seible, F. (2000). "Development of Performance Evaluation Database for Concrete Bridge Components and Systems under Simulated Seismic Loads", Earthquake Spectra, *Professional Journal of the Earthquake Engineering Research Institute*, **16**(2).

20. Maheri, M.R. (1990). "Engineering Aspects of Manjil, Iran Earthquake of June 20, 1990-A field Report by EEFIT", Earthquake Engineering Field Investigation Team, Institute of Structural Engineers, London.

21. Zand, K. (1999). "Seismic Vulnerability of Highway Bridges in Iran", *Proceedings of 3rd International Conference on Seismology and Earthquake Engineering (SEE3)*, **2**, 1015-1020.

22. JICA (2003). "The Comprehensive Master Plan Study on Urban Seismic Disaster Prevention and Management for the Greater Tehran Area in the Islamic Republic of Iran", JICA and Tehran Disaster Prevention and Management Center.

23. FEMA 356 (2000). "Pre-Standard and Commentary for the Seismic Rehabilitation of Buildings", Federal Emergency Management Agency, Prepared by American Society of Civil Engineers, Prepared for Federal emergency Management Agency.

24. Eurocode 8 (1996). Design Provisions for Earthquake Resistance of Structures, Part 2: Bridges.

25. FEMA 440 (2005). Improvement of Nonlinear Static Seismic Analysis Procedures, Prepared by: Applied Technology Council (ATC-55 Project), Prepared for Department of Homeland Security Federal Emergency Management Agency.

26. ASCE/SEI 41 (2007). Seismic Rehabilitation of Existing Buildings, American Society of Civil Engineers Reston, Virginia.

27. Elwood, K., Matamoros, A., Wallace, J., Lehman, D., Heintz, J., Mitchell, A., Moore, M., Valley, M., Lowes, L., Comartin, C., and Moehle, J. (2007). "Update to ASCE/SEI 41 Concrete Provisions, ASCE/SEI 41 Supplement 1", *Earthquake Spectra*, EERI, **23**(3), 493-523.

28. AASHTO (2007). AASHTO-LRFD Bridge Design Specifications, American Association of State Highway and Transportation Officials, 2007 Interim Revisions, Fourth Edition.

29. Caltrans (2006). Seismic Design Criteria, Version 1.4, California Department of Transportation.

30. ATC 32-1 (1996). Improved Seismic Design Criteria for California Bridges: Resource Document, Applied Technology Council.

31. AASHTO (2009). AASHTO Guide Specifications for LRFD Seismic Bridge Design, American Association of State Highway and Transportation Officials, First Edition.

32. Priestley, M.J.N., Seible, F., and Calvi, G.M. (1996). "Seismic Design and Retrofit of Bridges", Wiley, New York.

Notations

A_g = Column cross section area

f'_c = Compressive strength of unconfined concrete cylinder;

f_y = Yield strength of longitudinal bar;

f_{ye} = Expected yield strength of longitudinal bar;

l_{dh} = Basic development length of hooked bar;

d_b = Longitudinal bar diameter;

l_{ac} = Length of column reinforcement embedded into bent cap;

ρ_s = Volumetric ratio of spiral reinforcement to the confined core volume

ρ_s = Area ratio of longitudinal column reinforcement

D_C = Column confined core diameter

D_D = Seismic local or global displacement demand

D_C = Local or global displacement capacity

H_o = Column clear height;

μ_D = Ductility demand

ε_y = Longitudinal steel yield strain